Coastal Engineering, 15 (1991) 563–593
Elsevier Science Publishers B.V., Amsterdam

Laboratory measurements of uniform longshore currents

Paul J. Visser
Faculty of Civil Engineering, Delft University of Technology, P.O. Box 5048, 2600 GA Delft, The Netherlands

(Received May 22, 1990; accepted after revision January 17, 1991)

ABSTRACT

Visser, P.J., 1991. Laboratory measurements of uniform longshore currents. *Coastal Eng.*, 15: 563–593.

Experiments on uniform longshore currents in a wave basin are described. The measurements were performed in a basin with a pumped recirculation through openings in the wave guides. Minimal return flows in the offshore region of the basin are found to be accompanied with longshore currents which are virtually uniform alongshore. Three-dimensional longshore current velocity distributions were measured with much attention to quality control. Detailed experimental results are presented for different wave fields, two beach slopes and two beach roughnesses.

1. INTRODUCTION

When waves break obliquely to the shoreline a mean current is generated flowing parallel to the coast. These longshore currents play a significant role in the dispersion of pollutants and the erosion and deposition of sediment, and are therefore of great importance for managers of coastal areas, coastal engineers and marine geologists.

The theory of longshore currents has progressed considerably since the introduction of the concept of radiation stress by Longuet-Higgins and Stewart (1960, 1964), see the reviews by Longuet-Higgins (1972), Basco (1983) and Battjes (1988). The theoretical achievements obtained so far are considerable, although some of the assumptions are rather crude. These results call for a comparison with accurate experimental data, not only to evaluate the theoretical results but also to guide the process of improving theory. In addition, the theoretical longshore current models include coefficients which have to be determined from experimental data.

Measurements on longshore currents have been performed since 1949 both in the field (see the reviews by Galvin, 1967, Komar, 1975 and Basco, 1982)

and in the laboratory (Putnam et al., 1949; Brebner and Kamphuis, 1963; Galvin and Eagleson, 1965; Mizuguchi and Horikawa, 1978).

The uncontrollability of the circumstances and the variability of the observations in time and space are the main problems involved with longshore current measurements in the field. These problems can be met by recording simultaneously current velocities and sea surface displacements in many points in numerous locations. It is clear that such comprehensive field observations are very expensive. In this respect, reference is made to the extensive NSTS field observations (Seymour and Gable, 1980).

In the early laboratory observations of longshore currents only "the longshore current velocity" was measured, i.e., the averaged (over the surf zone width) current velocity or the maximum velocity. The data of these measurements are not appropriate for a comparison with the present longshore current theories.

Galvin and Eagleson (1965) measured the on–offshore variation of the longshore current velocity in several lines normal to the shoreline. Their data have revealed that there are also some difficulties with longshore current experiments in the laboratory. These problems are mainly caused by the finite length of a wave basin beach not permitting the current to reach its equilibrium profile, unless special precautions are taken.

Mizuguchi and Horikawa (1978), see also Kraus and Sasaki (1979), were the first (to the author's knowledge) to measure longshore current velocities in different points in the vertical. Because Mizuguchi and Horikawa (1978) used Galvin and Eagleson's (1965) wave basin geometry, their longshore current data reveal unfortunately also distinct alongshore variations and unrealistic large values for the flow velocities outside the breaker zone (see Section 5).

The lack of controlled longshore current data has motivated the author to perform detailed observations of longshore currents with much attention to the alongshore uniformity of the flow velocities and the accuracy of the measurements.

The objective of this paper is the presentation of a method developed to establish a longshore current in a wave basin, which is (virtually) uniform alongshore, and to give the main set of data of the uniform flow velocity observations. The data set includes a summary of experimental results reported before (Visser, 1982, 1984a) and new data (Experiment 8, angles of incidence in the nearshore zone). These data are presented here for use by others, not for use in the paper itself. The measurements were restricted to longshore currents generated by regular waves.

2. WAVE BASIN TYPE AND RECIRCULATION PROCEDURE

2.1 Choice of wave basin type

Figure 1 shows several wave basin types, which have previously been used in laboratory investigations on longshore currents:

(1) The completely enclosed wave basin (Putnam et al., 1949) in which the recirculation of the recirculation flow occurs in the offshore region of the basin.

(2) A basin with an opening in the downstream wave guide-wall and with a clearance under the wave board to allow recirculation (Galvin and Eagleson, 1965; Mizuguchi and Horikawa, 1978).

(3) A wave basin with surf zone openings in both wave guides to permit recirculation outside the wave guides, i.e., behind the wave generator or through a pipe under the beach (Brebner and Kamphuis, 1963). The recirculation is driven by the water level difference present between the downstream and updrift end of the basin beach.

(4) A basin as Type 3 but the recirculation occurs here both behind and beneath the wave board. This recirculation is enhanced by pumping in a small flow at the updrift wave guide (Kamphuis, 1977).

(5) A circular wave basin with a circumferential beach and a spiral wave maker operating in the centre of the basin (Dalrymple and Dean, 1972).

Boundary effects in wave basins are avoided with the spiral wave generator of the Type-5 basin. It can be a tool for longshore current studies if a much larger basin is used than the 5-m-diameter basin of Dalrymple and Dean

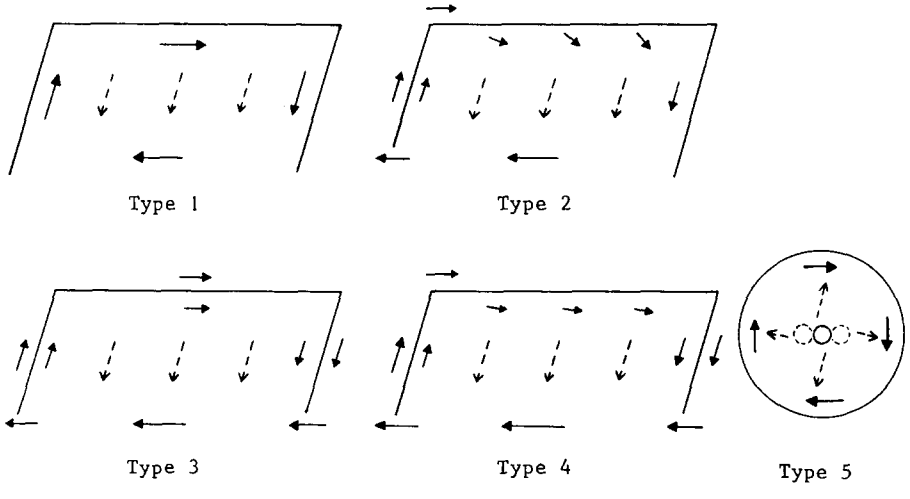

Fig. 1. Five types of wave basin set-ups (solid arrows denote flow rates, dashed arrows denote wave direction).

(1972). To the author's knowledge such a large circular wave basin has not been used to date.

Dalrymple et al. (1977) measured circulation streamlines and "longshore velocities along the surf zone" in the Types-1, -2 and -3 wave basins. They concluded that "the Type-3 basin would reduce the amount of return flow in the offshore region if a working recirculation procedure could be devised".

The clearance under the wave board in Type 4 allows a recirculation between the wave guides too. According to Kamphuis (pers. commun., 1985) this small recirculation has a stabilizing influence on the uniformity of the beach in longshore sand transport studies. However, it also means that the longshore current flow will increase in longshore direction and that the longshore current is not completely uniform. This consideration and the conclusion of Dalrymple et al. (1977) have led to the choice of a Type-6 basin for the present experiments (Fig. 2). Type 6 rests on Type 3, but holds the following adaptations:

(a) the external recirculation is completely effected and controlled by a pump;
(b) the width of the opening in the downstream wave guide is not necessarily equal to the surf zone width;
(c) an inflow distributor in the opening of the updrift wave guide (increases the length along which the longshore current is uniform).

The controllability of the inflow and outflow conditions is a strong asset of the Type-6 wave basin. However, the choice for this basin type also means that the following quantities have to be determined before starting the actual measurements (Fig. 2): the pumped recirculation flow rate Q_p; and the width w_d of the opening in the downstream wave guide. A recirculation scheme has

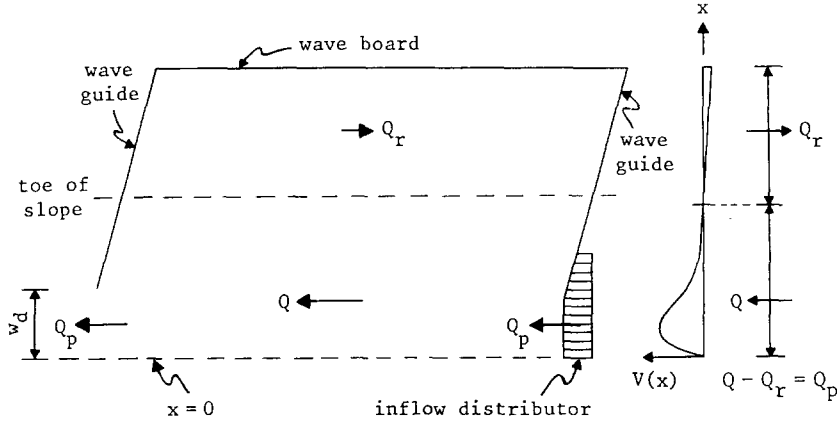

Fig. 2. Present wave basin set-up (Type 6).

to be developed to determine optimal values of these quantities so as to produce a longshore current with minimal deviations from uniformity.

2.2 Recirculation scheme

Figure 2 shows schematically wave basin Type 6. Q is the total longshore current flow rate, while Q_r is the return flow rate in the offshore region (or the internal recirculation flow rate). For continuity reasons:

$$Q = Q_p + Q_r$$

The depth contours of the sloping beach in the basin are parallel to the straight shoreline. It is assumed that the waves between the wave guides are uniform alongshore (apart from phase differences). From the equations describing conservation of mass and momentum (see e.g., Phillips, 1966) it follows that the depth-averaged longshore current velocity V in the wave basin is uniform alongshore if both (1) the slope of the mean water level in alongshore direction is zero and (2) the depth-averaged mean current velocity U in x-direction is zero (x is the coordinate in on–offshore direction).

It is, however, impossible to measure accurately mean water level slopes in the nearshore zone in a wave basin. This is caused by inevitable longshore variations of wave set-up and set-down (due to wave height variations). Also the condition $U=0$ is difficult to measure since the velocities in x-direction vary strongly with depth (due to the vertical variation of wave induced mass transport velocities in wave propagation direction) and are also relatively small.

Visser (1980, 1982) has proposed an alternative method to establish a longshore current in the wave basin which deviates minimally from alongshore uniformity. If Q_{pu} is the value of Q_p that goes with a nearly uniform longshore current flow rate Q_u, then the method is based on the assumption that Q_{pu} can be found by minimizing Q_r as function of Q_p (Fig. 3):

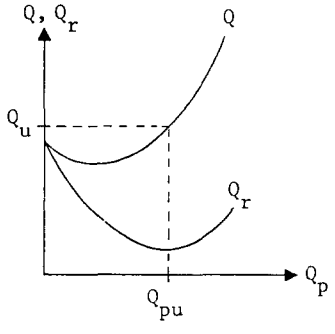

Fig. 3. Nearly uniform Q_u goes with minimal Q_r.

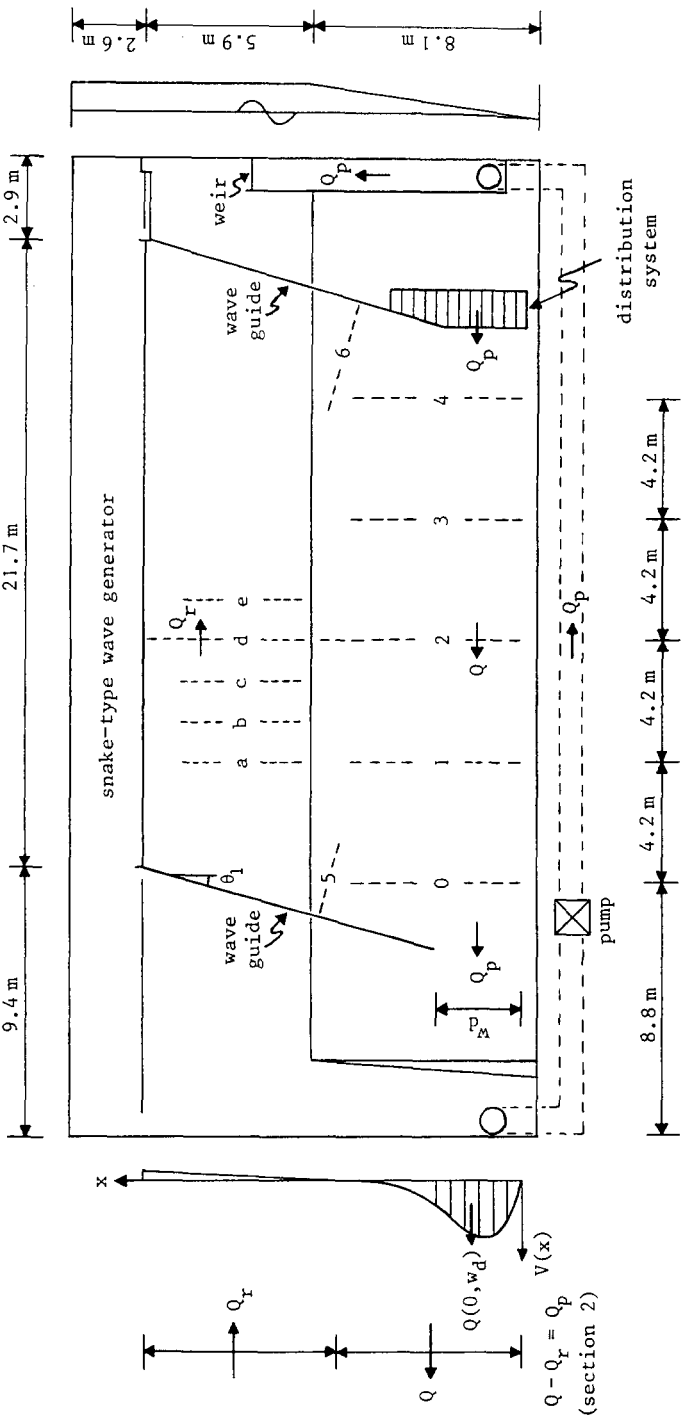

Fig. 4. Plan view of wave basin (slope 1:20).

(a) lower Q_p values will cause the flow rate Q to grow alongshore; the surplus $Q-Q_p$ returns offshore and raises Q_r;
(b) conversely, for $Q_p > Q_{pu}$ the excess will generate a circulation flow between the wave guides (by convection and lateral friction) which will also increase Q_r.

To verify this recirculation criterion, the pumped flow rate Q_p and the width w_d of the opening in the downstream wave guide were varied in the present experiments. The Types 1 and 3 basins were also investigated. The experiments are described in next chapter.

3. EXPERIMENTAL PROCEDURE

3.1 Experimental arrangement

The experiments were performed in the 34.00 m long, 16.60 m wide and 0.68 m deep wave basin of the Civil Engineering Faculty of the Delft University of Technology (see Fig. 4). The wave board of the snake-type wave generator consists of 0.40-m wide rubber pannels; only regular waves can be produced.

Concrete beaches with slopes 1:10 and 1:20 were constructed opposite to the wave generator. This was done carefully: in lines parallel to the wave board, still water depths varied only within ± 0.2 cm. The D_{90} of the roughness elements of the concrete beaches is estimated at $D_{90} \approx 0.6$ mm. For the final two experiments, the 1:20 slope was roughened by bonding 5–10 mm gravel ($D_{90}=8$ mm) with a thin grout on the concrete beach. The measuring sections and the horizontal positions of the measuring points were marked on the bottom. Figure 4 shows the positions of the sections 0, 1, 2, 3, 4, 5 and 6 and a, b, c, d and e. Wave guide-walls were composed of concrete elements and installed at angles of 15.4 or 31.0 degrees with the normal to the wave board.

The inflow distributor in the opening of the updrift wave guide consisted of twelve channels, each 0.20 m (1:10 slope) or 0.40 m (1:20 slope) wide, giving a total width of at least 1.7 times the width of the surf zone. The pumped flow rate Q_p was distributed in this system according to the expected distribution of the longshore current flow and was adjusted (with grids, slide-valves, etc.) if that turned out to be necessary.

3.2 Measuring procedure

The observations were started one hour after the start of wave generator and recirculation pump; these 60 minutes were sufficient to eliminate long-periodic start-related variations in flow and wave fields.

Current velocities were measured using dye ($KMnO_4$ dissolved in water,

yielding a fluid with a density practically equal to that of water). Dye was chosen based on an investigation by Delft Hydraulics Laboratory (1977), in which the application of floats, dye, a micro-propeller current meter and an Ott propeller current meter was examined. It was found that the miniature-propeller current meter gave 17% lower and floats 2% higher results than dye. Dye gave further the lowest variance.

Dye clouds were injected with a simple injection-apparatus mounted on a tripod, allowing an accurate positioning of the injection point. Dye injections took place at different waves phases for the five, ten or twenty independent readings per measuring point (see Table 1). This was done to eliminate as much as possible the influence of the orbital velocity on the measuring result. The travel times of the centres of clouds of dye were measured over distances varying between 0.30 m (current velocities smaller than 0.1 m/s) and 1.00 m (current velocities larger than 0.5 m/s). It was not possible to follow dye

TABLE 1

Summary of measuring procedure

Measure-ments of	Measuring method	Measuring sections (Fig. 4)	Horiz. distance between two measuring points	Number of observations/ observational time
Current velocity	dye ($KMnO_4$) in the vertical in three points	0, 1, 2, 3, 4	1:10 slope 0.20 m 1:20 slope 0.40 m (0.20 m near shoreline)	surf zone: 20 per point (60 per vertical) outside surf zone: 10 or 5 per point
Wave height	resistance wave probes	1, 2	0.20 m	90 seconds
		a, b, c, d, e	0.20 m (20 points per section)	
		3–5 sections on and near the breaker line	0.20 m (29 points per section)	
Mean water level	bottom pressure tappings	1, 2	1:10 slope 0.20 m 1:20 slope 0.40 m (0.20 m in surf zone)	
Position of plunge line	visually	near 1 and 2	0.40 m (6 points)	5 per point
Angle of incidence	wave probes	constant depth part of basin		
	photograph	nearshore zone	1:10 slope 0.20 m 1:20 slope 0.40 m	about 20
Wave run-up	visually	between 1 and 2	0.40 m (12 points)	5 per point

clouds in the surf zone over distances exceeding about 1.0 m because of the fast spreading of the dye by turbulence. To secure accuracy, the velocity observations in the surf zone were conducted by two persons and the number of observations per measuring point was enlarged from ten to twenty. Spreading of dye clouds was small outside the surf zone; one person could perform the measurements in this region.

The current velocity observations were done at three levels in the vertical: at the surface, at mid-depth and near the bottom (i.e., 1.0 cm above the bottom). This allows an estimate of the vertical structure of the time-averaged velocity and a more accurate determination of the depth-averaged current velocities than measurements taken at a single elevation. The depth-averaged current velocity V was determined as:

$$V = (v_{\text{surface}} + 2\, v_{\text{mid-depth}} + v_{\text{bottom}})/4$$

Besides Mizuguchi and Horikawa (1978) and the author, also Kim et al. (1986) have measured longshore current velocity distributions in the vertical.

The height of periodic (mechanically generated) waves varies in a wave basin also in the constant-depth part of it. Wave reflection against the beach, reflection of these reflected waves once again against the wave guides and the wave board, as well as super- and subharmonic waves cause a variation of wave heights both in on–offshore direction (as in a wave flume) and in alongshore direction (about $\pm 10\%$ in the present wave basin). In the constant-depth part of the basin, wave height was measured in five sections (a, b, c, d and e) and in each section in about twenty points. Averaging over about 100 measuring points gave an accurate value for the wave height in the flat part of the basin (i.e., with an inaccuracy of about $\pm 2\%$).

To determine the alongshore-averaged breaker height and position of the breaker line, wave heights were measured in three to five sections parallel to the shoreline (see Table 1). A breaker point is here defined as the point in a cross-shore section, being located at or just shoreward of maximum wave height, where the wave height starts to decrease significantly. Alongshore averaging over 29 measured breaker point positions gave the x-coordinate of the breaker line.

For measurements of mean water level change, pressure tappings were provided (inner diameter 2 mm), flush with the smooth concrete bottom, see Table 1. The tappings were connected with plastic tubes to stilling wells (inner diameter 10 cm), where the static head was measured with a point gauge with an inaccuracy of ± 0.01 cm. Mean water level variations were not measured in the experiments on the rough bottom. Instead, data from experiments on the smooth concrete bottom with similar wave fields were adopted.

In a plunging breaker the wave crest curls at the breaker line over the front face of the wave and falls next into the trough water ahead, resulting in a high splash and the development of a bore-like wave front (Galvin, 1968). The

point where the curly crest impinges on the preceding wave trough is defined as the plunge point. An accurate measurement of the position of the plunge line (in six measuring points, see Table 1) was difficult: individual observations could be made with an inaccuracy of approximately ± 5 cm.

In the constant-depth part of the basin, angles of incidence were measured with three wave probes. Accurate results (i.e., with an inaccuracy of about ± 0.5 degrees) could be obtained directly after the start of the wave generator, when waves of nearly constant form were present. In the nearshore zone, angles of incidence were measured by photograph, with the camera at a height of 5.5 m above the waves. Both observer variation and distortion by photo method were checked. The inaccuracy of the results of these observations is estimated at ± 1.5 degrees.

3.3 Experimental program

The beach and input wave conditions are given in Table 2, where α is the slope angle, T is the wave period, d is the still water depth, θ is the angle of incidence, H is the wave height, λ is the wave length, 'pℓ' means plunging breakers and 'sp' stands for spilling breakers; the indices 0 and 1 refer to values on deep water and constant-depth part of the basin, respectively.

H_0 and θ_0 were calculated from H_1, θ_1 and T using first-order cnoidal wave theory (Svendsen and Hansen, 1977) for Experiments 1, 5 and 8, where $d_1/\lambda_0 < 0.1$, and linear wave theory for Experiments 2, 3, 4, 6 and 7, where $d_1/\lambda_0 > 0.1$.

Experiment 6 was started with spilling-type breakers. But the wave field in the basin with these breakers was pretty unstable and nonuniform in longshore direction. Hence, the experiment was performed with somewhat lower

TABLE 2

Beach and input wave conditions

Exp. no.	tan α	T (s)	d_1 (cm)	θ_1 (degr)	H_1 (cm)	H_0 (cm)	$\frac{H_0}{\lambda_0}$	θ_0 (degr)	Breaker type
		Smooth conrete beach							
1	0.101	2.01	39.9	31.1	7.2	11.3	0.018	62.0	pℓ
2	0.101	1.00	39.9	30.5	9.5	10.2	0.065	32.5	pℓ
3	0.101	1.00	40.1	15.4	8.9	9.6	0.062	16.4	pℓ
4	0.050	1.02	35.0	15.4	7.8	8.5	0.052	17.0	pℓ
5	0.050	1.85	34.8	15.4	7.1	8.0	0.015	26.6	pℓ
6	0.050	0.70	35.0	15.4	5.9	6.0	0.078	15.5	sp/pℓ
		Gravel beach							
7	0.050	1.02	35.0	15.4	7.8	8.5	0.052	17.0	pℓ
8	0.050	1.85	35.0	15.4	7.1	8.0	0.015	26.6	pℓ

TABLE 3

Summary of program of current velocity measurements

Exp. no.	Beach	tan α	Wave basin type	Width opening in upstream wave guide	$\frac{w_d}{x_{br}}$	Q_p (dm^3/s)	Measuring sections for current velocity observations (Fig. 4)		Q_{pu} (dm^3/s)
1A	smooth concrete	0.101	6	1.3 x_{br}	1.0	0,15,20,25,30,35,40	2,d		
				1.3 x_{br}	1.15	0,17,25,30,35,40,48	2,d,5,6		
				1.3 x_{br}	1.3	30,35,40	2,d,5,6	0,1,2,3,4	35
				1.3 x_{br}	1.45	25,30,35,40,45,50	2,d		
				1.3 x_{br}	2.0	30,35,42,59	2,d,5,6		
1B	0.101		6	distr. syst.	1.0	25	2,d		
				distr. syst.	1.15	30	2,d		
				distr. syst.	1.3	25,30,35,40,45,50	2,d,5,6	0,1,2,3,4	35
				distr. syst.	1.45	40	2,d		
				distr. syst.	1.6	45,50	2,d		
1C	0.101		1	0	0	0	0,1,2,d,3,4,5,6		–
1D	0.101		3	1.0 x_{br}	1.0	12 (="free Q_p")	0,1,2,d,3,4,5,6		–
2	0.101		6	distr. syst.	1.2 to 1.4	20,30,35,40[A],45,50,60[A],70	2,d	0,1,2,3,4	50
3	0.101		6	distr. syst.	1.3 to 1.5	10,20,30[B],40,50[B],60,70,80	2	0,1,2,3,4	40
4		0.050	6	distr. syst.	1.2 to 1.3	30,40,50,60,70,80	2	0,1,2,3,4	50
5		0.050	6	distr. syst.	1.3	40,50,60,65,70,80	2	0,1,2	65
6		0.050	6	distr. syst.	1.35	30	2	0,1,2	30
7	gravel	0.050	6	distr. syst.	0.9 to 1.1	10,15,20,25,35,45	2	0,1,2,3	20
8		0.050	6	distr. syst.	1.2	25		2	25
						for minimizing Q_r or $Q-Q_p$		virtually uniform longshore currents	

[A] for $Q_p = (1 \pm 0.20) Q_{pu}$ also observations in sections 0, 1, 3 and 4.
[B] for $Q_p = (1 \pm 0.25) Q_{pu}$ also observations in sections 0, 1, 3 and 4.

waves, yielding breakers of the transitional form spilling/plunging (Galvin, 1968) with which the wave field in the basin was stable and more or less uniform alongshore.

A summary of the program of the current velocity measurements is given in Table 3. A total number of 75 different combinations of beach and wave conditions, wave basin geometries and flow rates Q_p has been tested. For the verification of the proposed recirculation criterion, wide ranges for Q_p and w_d/x_{br} have been used; x_{br} is the width of the breaker zone between wave set-up line ($x=0$) and breaker line ($x=x_{br}$).

In Experiment 1 current velocity observations were done in both section 2 and section d, and return flow rates could be determined (from the depth-averaged current velocities and mean water depths) directly as Q_r and indirectly as $Q-Q_p$. By comparing $Q-Q_p$ with Q_r each measurement could be checked (see par. 4.1). It turned out that the current velocity observations in section d were not really necessary and in Experiment 2 moreover hindered by irregular distributions of the current velocity in the vertical in the offshore region (Visser, 1982). Consequently, these observations were no longer done in subsequent experiments.

4. EXPERIMENTAL RESULTS

4.1 Verification of recirculation criterion

Figure 5 shows the flow rates Q and $Q-Q_p$ in Experiment 1A (in which no inflow distributor was used). A minimal $Q-Q_p$ was found for $Q_p=35$ dm^3/s and $w_d/x_{br}=1.3$, yielding a virtually uniform longshore current flow, see Fig. 6 (where Q_s is the surf zone flow rate between $x=0$ and $x=x_{br}$, and Q_{2s} is the alongshore flow rate between $x=0$ and $x=2x_{br}$). The results of this experiment have also revealed (Visser, 1982) that $Q-Q_p$ was minimal for given Q_p if w_d was chosen such that the longshore current flow rate in section 2 between $x=0$ and $x=w_d$ was equal to Q_p. So in Experiments 1B and 2–8, w_d was varied in this way (Table 3). The minimal $Q-Q_p$ in Experiment 1B was also found for $Q_p=35$ dm^3/s and $w_d/x_{br}=1.3$. The main effect of the inflow distributor was an increase of the length along which the longshore current was uniform (Visser, 1982).

Figure 7 shows Q and $Q-Q_p$ in Experiment 2. A minimum $Q-Q_p$ was found for $Q_p=50$ dm^3/s and $w_d/x_{br}=1.3$, again inducing a nearly uniform longshore current (Fig. 8). Figure 8 also shows that even a relatively small deviation of 20% in Q_p from Q_{pu} results in a significant deviation from uniformity of the longshore current flow along the basin beach. Experiment 3 has similar results (Visser, 1982).

Experiments 1, 2 and 3 confirm the proposed recirculation scheme for the Type 6 wave basin. The procedure was succesfully applied in Experiments 4,

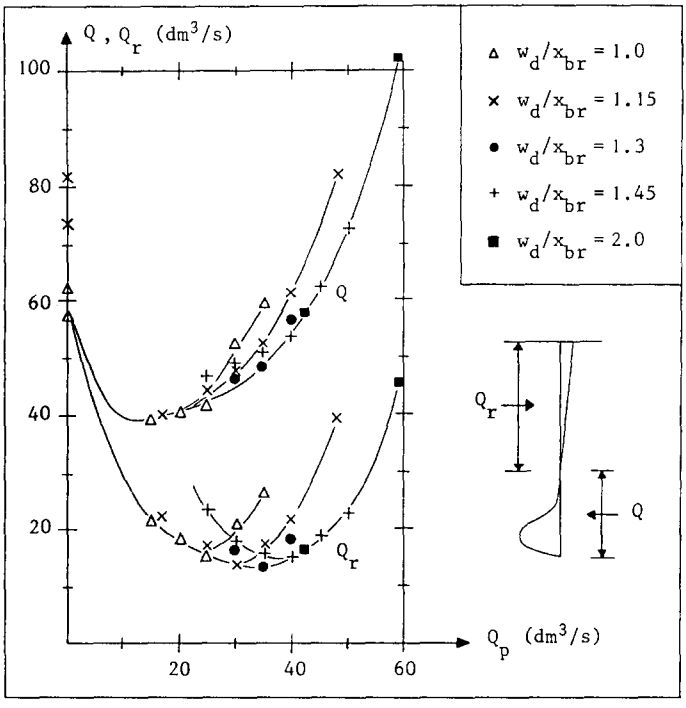

Fig. 5. Q and Q_r in sections 2 and d for different Q_p and w_d/x_{br} in Experiment 1A.

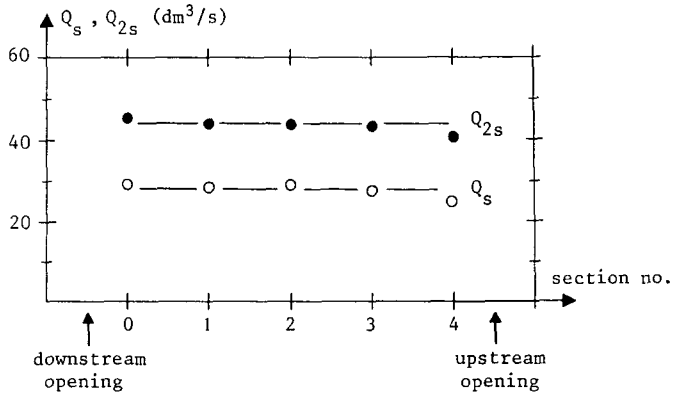

Fig. 6. Q_s and Q_{2s} along the basin beach for $Q_p = 35$ dm^3/s and $w_d/x_{br} = 1.3$ in Experiment 1A.

5 and 7 (Visser, 1982): the minimal $Q - Q_p$ gave always the most nearly uniform longshore current flow.

Figure 8 indicates that it is also possible to establish a virtually uniform longshore current in a wave basin by comparing Q_{2s} in two different sections, for instance sections 0 and 2. If Q_{2s} in section 2 is larger than in section 0 then

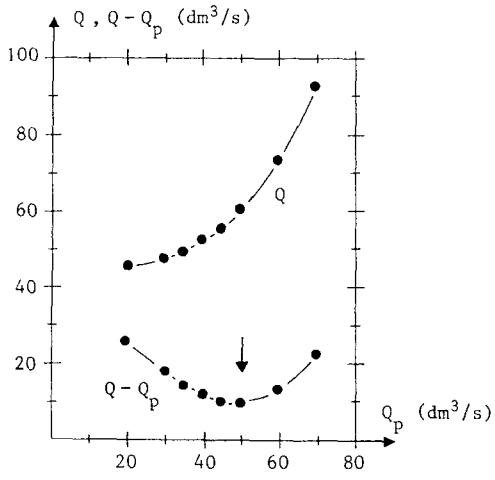

Fig. 7. Q and $Q-Q_p$ in section 2 for different Q_p and for w_d/x_{br} varying between 1.2 and 1.4 in Experiment 2.

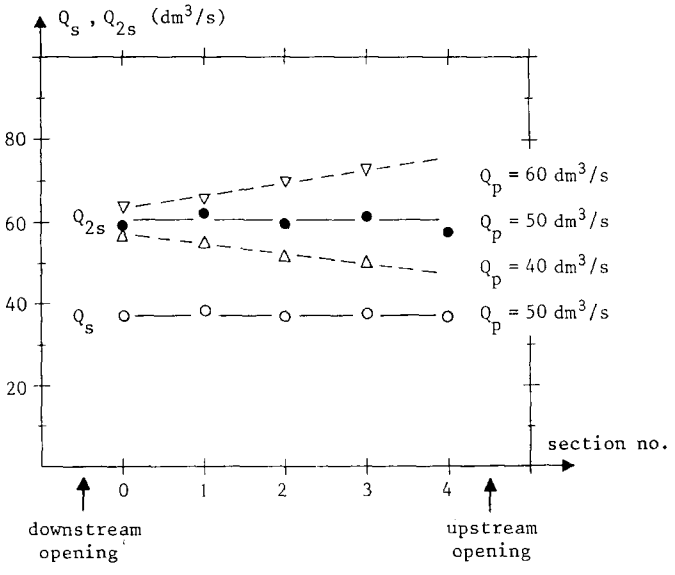

Fig. 8. Q_s and Q_{2s} along the beach for $Q_p=50$ dm^3/s and $w_d/x_{br}=1.3$ in Experiment 2; Q_{2s} also for $Q_p=40$ dm^3/s and $Q_p=60$ dm^3/s.

$Q_p > Q_{pu}$ and conversely, if Q_{2s} in section 2 is smaller than in section 0 then $Q_p < Q_{pu}$. A mixture of luck and some experience led to a first choice of $Q_p=30$ dm^3/s in Experiment 6, that yielded a nearly uniform longshore current (Visser, 1982). Hence, only observations with $Q_{pu}=30$ dm^3/s were done in this experiment, see Table 3. However, in general this method will require more

measurements compared with minimizing $Q-Q_p$ in section 2, since observations in two sections are required instead of one.

In Experiment 8, flow velocity observations were only performed in section 2 with $Q_p=25$ dm^3/s, assuming this was Q_{pu} (see Table 3). For the determination of this value for Q_{pu} it was assumed that the ratio between Q_{pu} in Experiment 8 and in Experiment 7 is equal to that of it in Experiment 5 and in Experiment 4 with similar wave fields, respectively (see Table 2).

Observations in the Types 1 and 3 wave basins, shown in Fig. 1, were done to examine the sensitivity of the longshore current for the wave basin geometry, see also Visser (1980). Figures 9 and 10 show the results for Q_s and Q_{2s}. The longshore currents were clearly nonuniform alongshore, while the uniform longshore current profile of Experiments 1A and 1B was not present in any section.

The recirculation between the wave guides in the Type-1 basin caused a substantial exaggeration of Q and Q_r: $Q=128$ dm^3/s and $Q_r=135$ dm^3/s, while

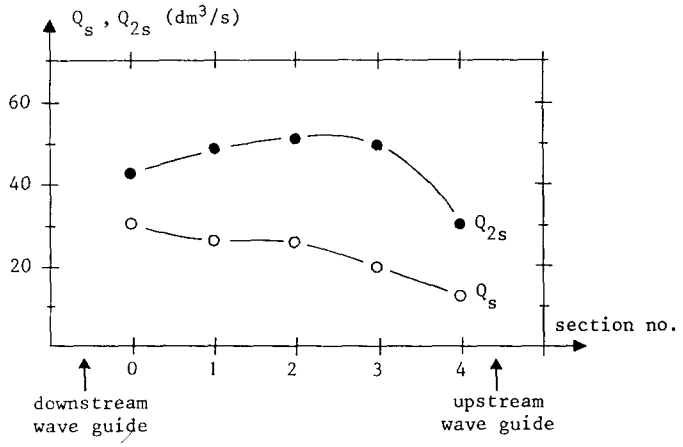

Fig. 9. Q_s and Q_{2s} along the beach in Type-1 wave basin (Experiment 1C).

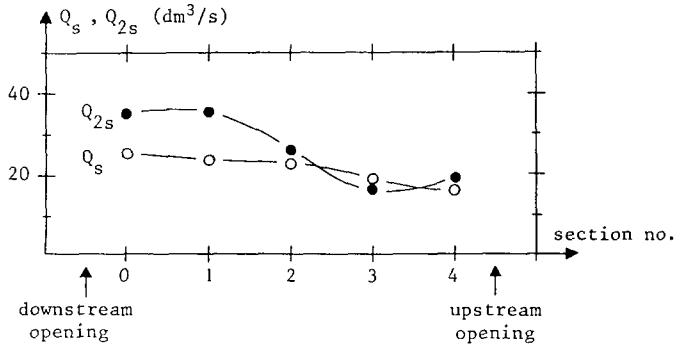

Fig. 10. Q_s and Q_{2s} along the beach in Type-3 wave basin (Experiment 1D).

in Experiments 1A and 1B: $Q=50$ dm^3/s and $Q_r=15$ dm^3/s for $Q_p=35$ dm^3/s. In Experiment 1D: $Q=25$ dm^3/s, $Q_r=10$ dm^3/s and the external recirculation flow rate $Q_p=12$ dm^3/s.

The observations in the basin Types 1 and 3 clearly show that these wave basins are not appropriate for detailed measurements of uniform longshore currents, and this is also the case with Type 2 (see Section 5).

Adding all $Q-Q_p$ and all Q_r measured in Experiments 1A and 1B gives $\Sigma(Q-Q_p)=2167-1241=926$ dm^3/s and $\Sigma Q_r=935$ dm^3/s. The difference of 9 dm^3/s is only 0.4% of ΣQ and 1.0% of $\Sigma(Q-Q_p)$. So, the systematic error in the current velocity observations is very small. However, per measurement the difference between $Q-Q_p$ and Q_r is not always small (Visser, 1982): a typical value for this difference is 10% of $Q-Q_p$. It is expected that the differences between $Q-Q_p$ and Q_r are largely due to the less accurate measurement of Q_r (rougher measuring grid, less observations per point, see Table 1) and that the $Q-Q_p$ values are more accurate values for the rates of return flows than the Q_r values.

4.2 Wave and mean water level data

A summary of the output wave data is given in Table 4; γ is the surf zone averaged value of H/h, where h is the mean water depth $=d+\eta$, η is the wave set-up or set-down, η_m is the maximum value of the wave set-up, R is the wave run-up and the indices br and pℓ refer to values on the breaker line and the plunge line, respectively. These data were obtained in the situations with virtually uniform longshore currents.

The results for γ and R/H_0 agree with data obtained by many researchers in wave flumes ($\theta=0$), see e.g., Battjes (1974). The parameter:

$$\xi_{br}=\frac{\tan\alpha\cos\theta_{br}}{\sqrt{H_{br}/\lambda_0}}$$

TABLE 4

Summary of output wave data

Exp. no.	H_{br} (cm)	d_{br} (cm)	$\frac{H_{br}}{d_{br}}$	γ	η_{br} (cm)	θ_{br} (degr)	$\theta_{p\ell}$ (degr)	$d_{p\ell}$ (cm)	x_{br} (cm)	$x_{p\ell}$ (cm)	η_m (cm)	R (cm)	Breaker type	ξ_{br}
1	10.5	10.4	1.00	1.18	−0.23	21.1	18.8	4.4	145	85	4.2	7.2	pℓ	0.73
2	10.0	10.9	0.91	0.82	−0.11	24.1	22.0	5.1	136	78	2.8	4.1	pℓ	0.36
3	9.7	11.4	0.85	0.82	−0.19	12.7	10.8	5.8	141	85	2.7	4.1	pℓ	0.40
4	9.1	11.0	0.83	0.56	−0.12	12.7	11.4	8.0	251	192	1.6	1.9	pℓ	0.21
5	10.8	11.6	0.93	0.75	−0.12	12.2	10.6	8.1	279	210	2.4	3.1	pℓ	0.35
6	5.8	8.8	0.66	0.50	−0.05	13.1	12.1	6.7	194	153	1.0	1.1	sp/pℓ	0.18
7	9.0	12.2	0.74	0.50	–	12.8	11.6	9.2	272	214	–	–	pℓ	0.21
8	10.8	12.2	0.89	–	–	–	–	8.8	292	220	–	–	pℓ	0.35

is the inshore surf similarity parameter of Battjes (1974), adapted to the oblique incidence (term cos θ_{br}). The present experiments indicate for the breaker type discriminator ξ_{br} between spilling and plunging breakers a value $\xi_{br}=0.2$. This is somewhat lower than the value given by Battjes (1974) using Galvin's (1968) data.

The breaker line and plunge line have already been defined in 3.2. The ratio of the width of the plunge travel region $x_{br}-x_{p\ell}$ to the mean breaker depth h_{br} can be calculated from Table 4; the value for this ratio varies between 4.7 and 6.0, which is in accordance with the wave flume data of Singamsetti and Wind (1980).

The mean water level was virtually constant between breaker line and plunge line as can be seen from Fig. 11. This figure shows the paradoxical fact already pointed out before (Battjes, 1972; Mizuguchi and Horikawa, 1978; Svendsen, 1984) that in the transition region (that is the zone just shoreward from the breaker line, where the wave shape changes rapidly) the radiation normal stress component S_{xx} is nearly constant even with a 30 to 60% decrease in wave height, see Fig. 12. This is not only the case in plunging breakers but also in spilling-type breakers, see for instance the observations of Hansen and Svendsen (1979) and Singamsetti and Wind (1980).

Figure 12 shows also Stive's (1984) theoretical (from a hydraulic jump formulation) curves for H/H_{br} as function of h/h_{br}. The agreement with the present data is fair. Near the water line the model of Stive overestimates the wave height. Svendsen (1984) has presented a similar model.

Figure 13 shows the measured $\sin\theta/\sin\theta_1$ versus $(c+V\sin\theta)/c_1$, in which V and θ were adopted from the data and where the wave phase velocities c and c_1 were calculated with first-order cnoidal wave theory (see Svendsen and Hansen, 1977) if $d/\lambda_0<0.1$ and with linear wave theory if $d/\lambda_0>0.1$. The scatter around the line $\sin\theta/\sin\theta_1=(c+V\sin\theta)/c_1$ is both due to measuring inaccuracies and the application of imperfect wave theories; the S-shape for $\sin\theta/\sin\theta_1\approx 0.85$ is due to the transition applying linear wave theory to first-order cnoidal wave theory. With values for $(V\sin\theta)/c$ increasing to about 0.1 inside the surf zone (in Experiments 1 and 2 even to about 0.4), the effect of current refraction is not always negligible.

4.3. Uniform flow velocity data

Two typical examples of the results of the longshore current velocity observations in the vertical are shown in Fig. 14 alongshore-averaged (justified because of near-uniformity). The flow velocities $v(z)$ were nearly constantly distributed over depth and clearly not with a logarithmic profile. This is in accordance with the data of Mizuguchi and Horikawa (1978) and Kim et al.

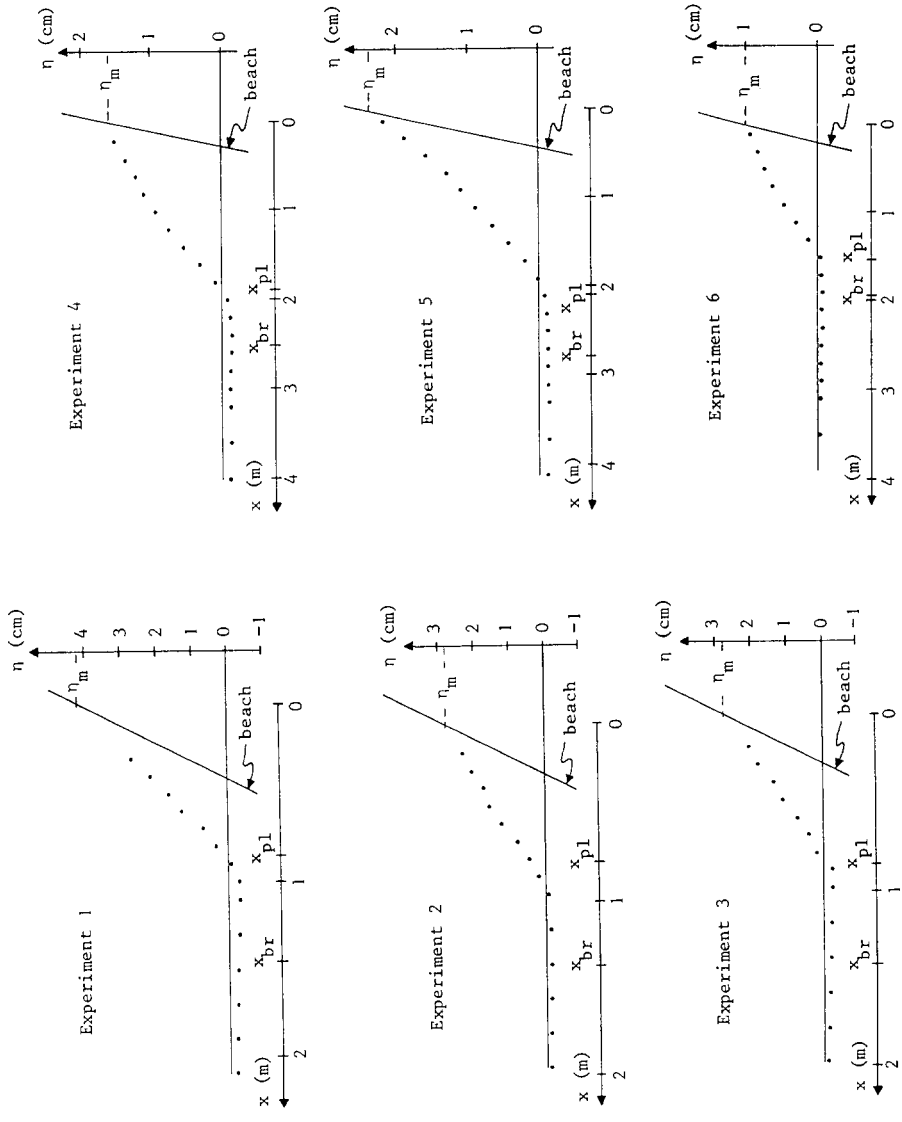

Fig. 11. Measured wave set-up and set-down η (alongshore-averaged over sections 1 and 2).

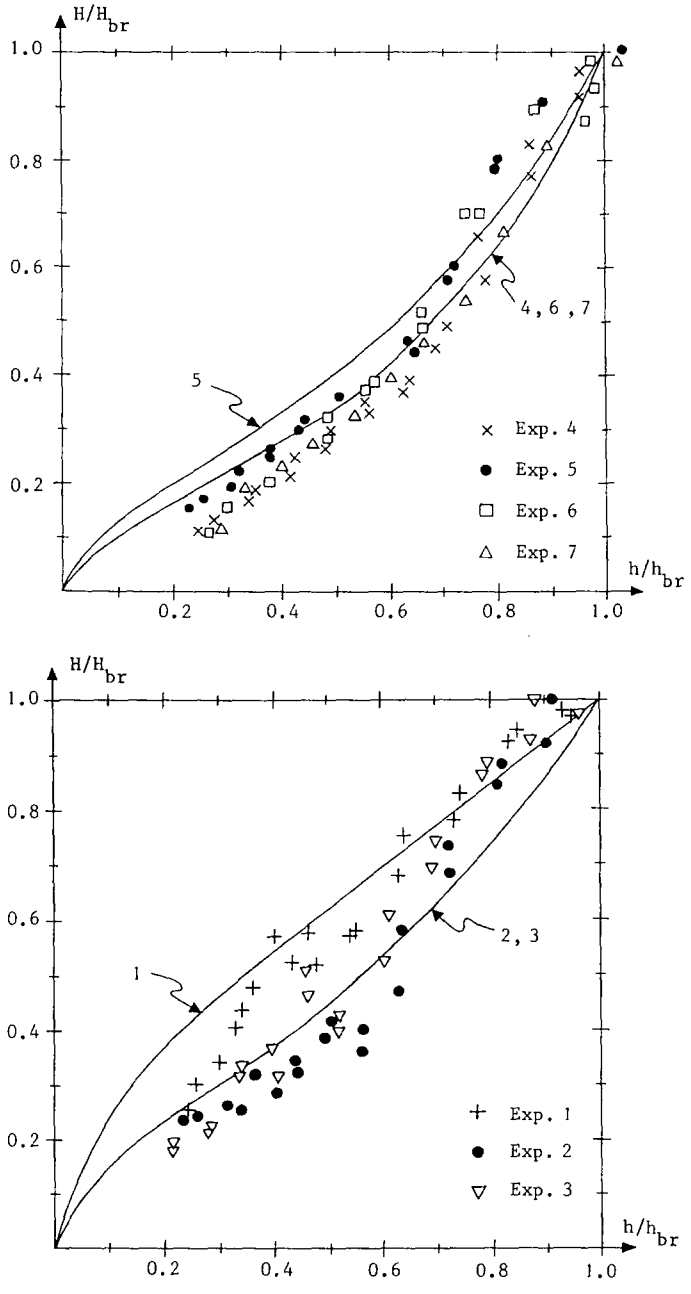

Fig. 12. Measured and theoretical (Stive, 1984) H/H_{br} as function of h/h_{br}.

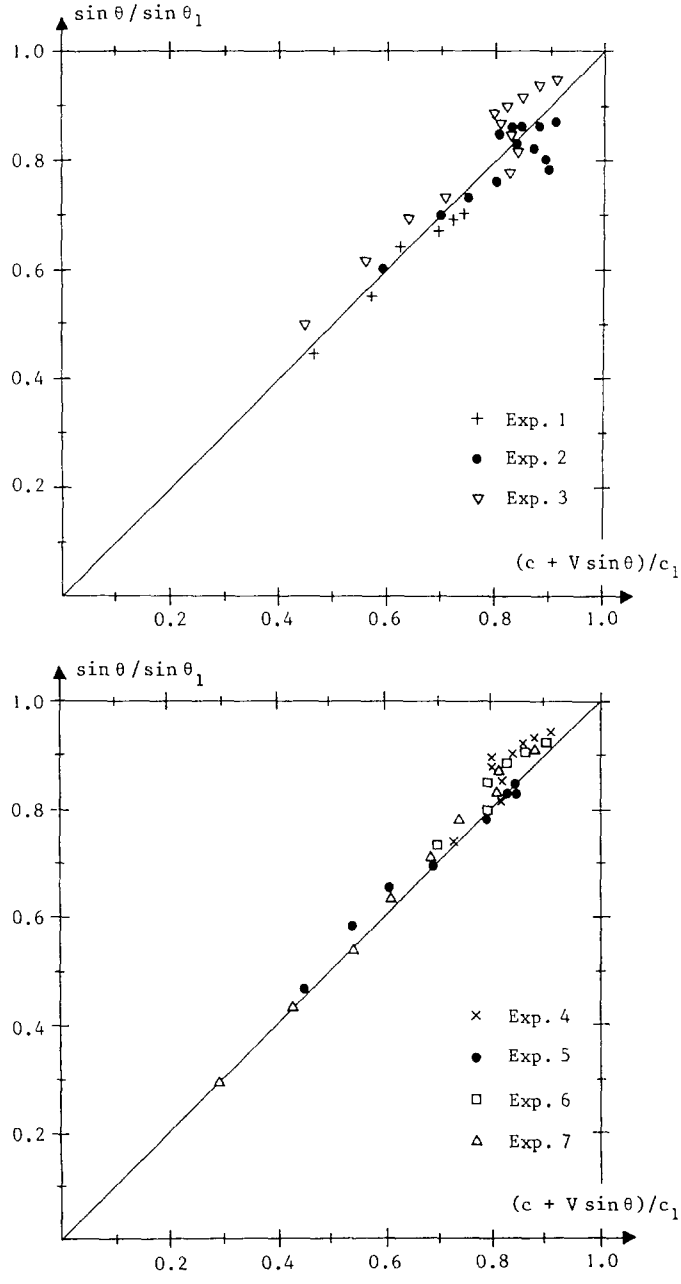

Fig. 13. Measured $\sin\theta/\sin\theta_1$ versus $(c+V\sin\theta)/c_1$.

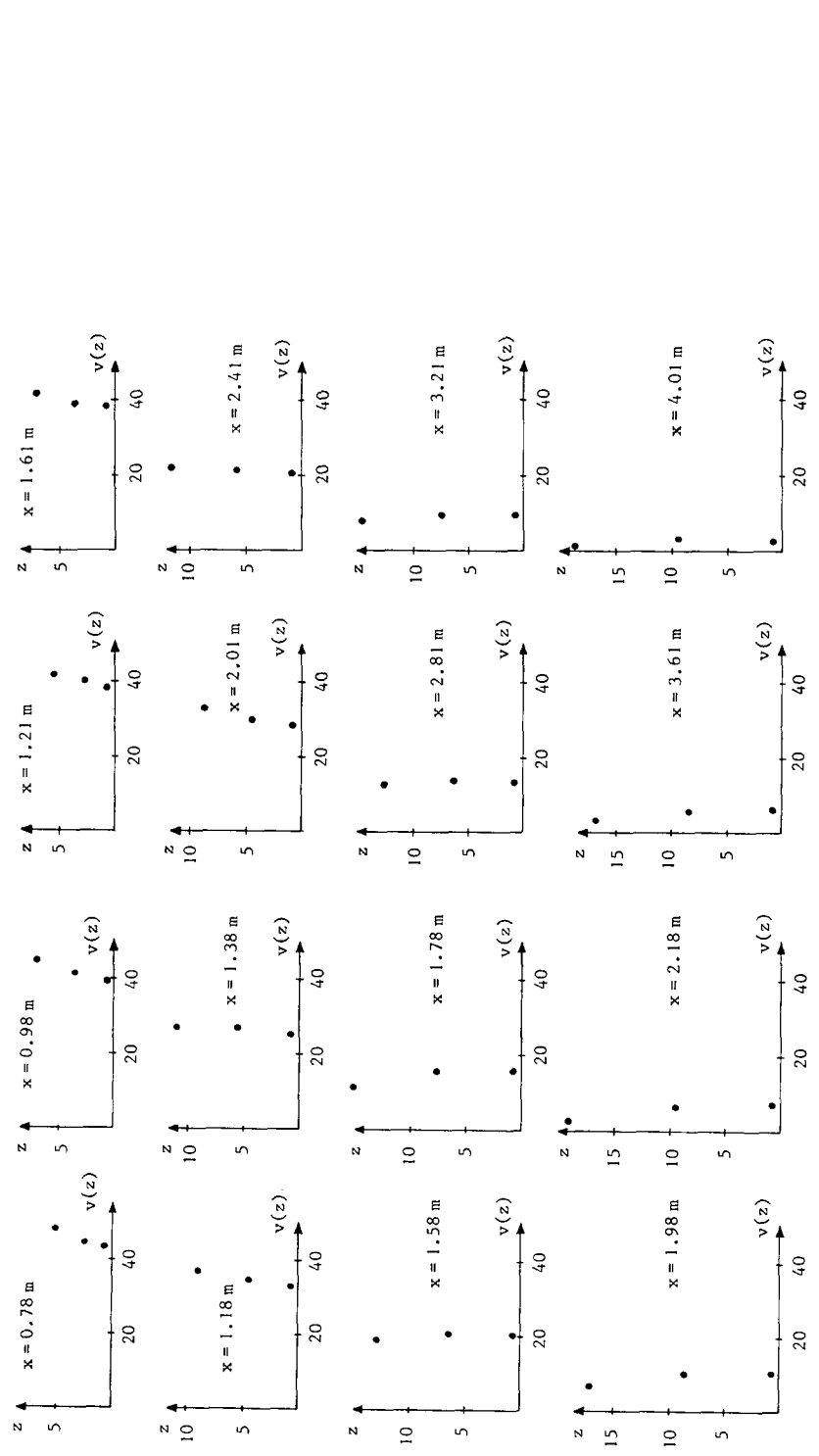

Fig. 14. Alongshore-averaged longshore current velocities $v(z)$ at three elevations z from the bottom (alongshore-averaging over the sections 0 through 3, z in cm, $v(z)$ in cm/s).

(1986). Interestingly, Svendsen and Lorenz (1989) recently presented a theoretical model which predicts a more or less constant velocity over depth.

The depth-averaged longshore current velocities $V(x)$ in the uniform situations are presented in Tables A-1 through A-8 in the Appendix. In spite of the inflow distributor, the current velocities in section 4 differed somewhat from the uniform values (see Figs. 15 and 16), and these data have not been included in the tables. Both Tables A-1 through A-7 and Figs. 15 and 16 show that the uniformity of the longshore currents from section 3 or 2 to section 0 is satisfactory. The tables in the Appendix include further the alongshore-averaged longshore current velocities $\bar{V}(x)$, the wave heights $H(x)$ and mean water depths $h(x)$ averaged over sections 1 and 2 and the angles of incidence $\theta(x)$.

In par. 4.1 it has already been stated that the systematic error in the current velocity observations is small. By taking numerous series of twenty readings in a point inside the surf zone and of ten readings outside, the random error of the current velocity observations in one measuring point could be determined at about $\pm 4\%$. This gives for the depth-averaged flow velocity a ran-

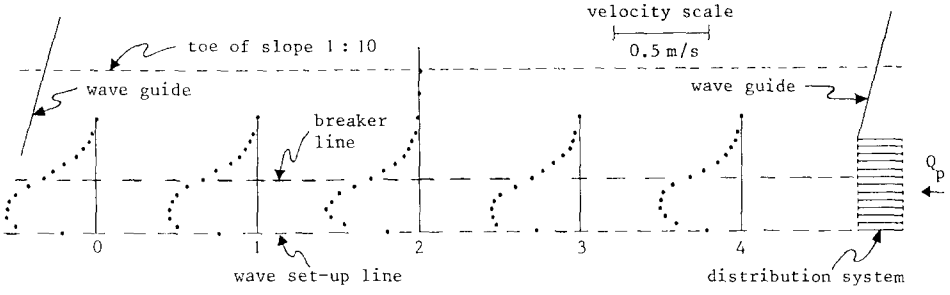

Fig. 15. Depth-averaged longshore current velocities V in uniform situation of Experiment 3 ($Q_p = 40\ \mathrm{dm^3/s}$, $w_d/x_{br} = 1.4$).

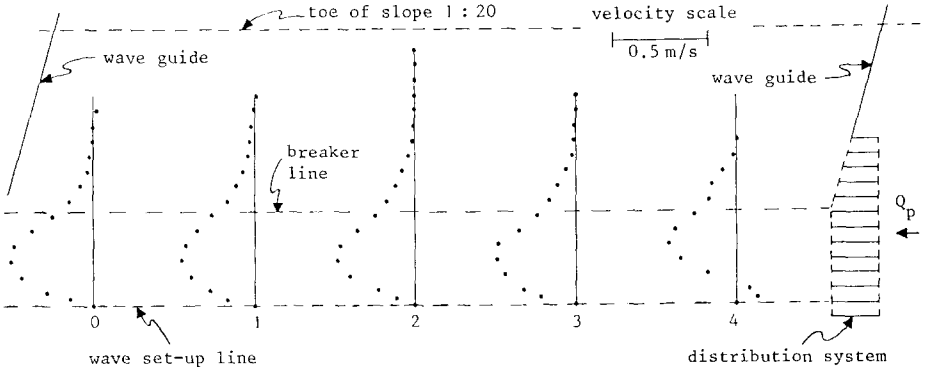

Fig. 16. Depth-averaged longshore current velocities V in uniform situation of Experiment 4 ($Q_p = 50\ \mathrm{dm^3/s}$, $w_d/x_{br} = 1.2$).

dom error of about $\pm 2.5\%$, which is surprisingly small considering the measuring technique (dye).

5. DISCUSSION

The ratio of basin width and basin length (measured between the wave board and shoreline, and the wave guides, respectively) is in the present wave basin about 2/3 (see Fig. 4). One can imagine that in a wave basin, with a larger value for this ratio, a second or even a third circulation cell can develop between the wave guides. Figure 17 shows an example: the return flow Q_r drives a second circulation Q_c. It is expected from the present study that also in this case a minimal return flow rate $Q_r = Q - Q_p$, as defined in Fig. 17, will be accompanied with virtually uniform longshore currents. As a matter of fact, a small second circulation ($Q_c \approx 2$ dm^3/s) was observed in some of the situations of Experiments 1A and 2. In experiment 1D in the Type-3 basin, Q_c was even relatively strong, i.e., $Q_c \approx Q_r$ (Visser, 1982).

The present method for establishing nearly uniform longshore currents in the Type 6 basin requires:

(a) velocity measurements in a cross-section near the centre of the basin beach for five or six different values of Q_p; three different measuring points in the vertical are sufficient to determine the depth-averaged flow velocities (because of the almost uniform distribution over depth) and about fifteen different horizontal positions in the section are necessary to obtain accurate values for $Q - Q_p$;

(b) mean water level observations in the same cross-section; since the wave set-up in the basin is not very sensitive for Q_p, it is not necessary to repeat these measurements for every Q_p.

These preliminary measurements can be done in a relatively short period

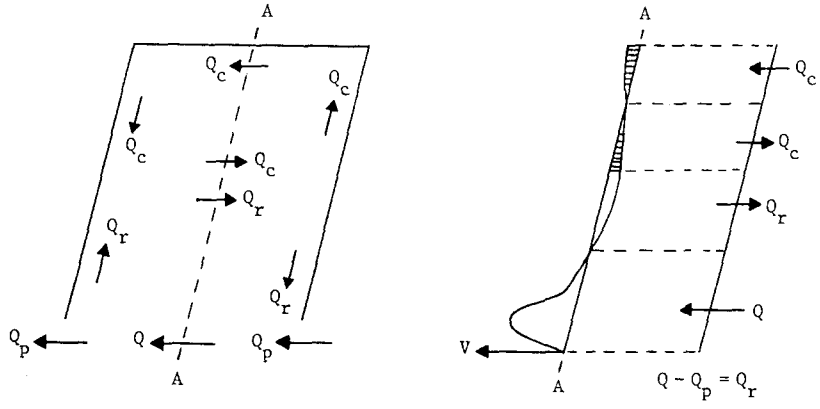

Fig. 17. Return flow Q_r drives a second circulation cell with flow rate Q_c.

of time and are essential if uniformity is of importance: the longshore current velocities in a basin can deviate substantially from the uniform values if Q_p/Q_{pu} differs well from unity.

Flow velocity observations in two extra cross-sections should be done in the situation where $Q-Q_{pu}$ is minimal to demonstrate the alongshore uniformity of the flow field. Since small alongshore variations in the longshore current velocities are inevitable, observations in different cross-sections also allow alongshore-averaging and thus provide more accurate data.

How do the present experimental results compare with the Type-2 basin data of Galvin and Eagleson (1965) and Mizuguchi and Horikawa (1978)? Figure 18 shows typical cross-sectional distributions of dimensionless flow velocities V/V_{max} (where V_{max} is the maximal flow velocity in the measuring section) in Galvin and Eagleson's (1965) and Mizuguchi and Horikawa's (1978) data compared with the cross-sectional distribution of V/V_{max} in present Experiment 4. Figure 18 illustrates that both Galvin and Eagleson (1965) and Mizuguchi and Horikawa (1978) measured longshore current velocities in the region well outside the surf zone which are significantly larger than in the present experiments. A similar cross-sectional flow velocity distribution (as that observed by Mizuguchi and Horikawa) was observed in the present Experiment 1C in the Type 1 basin (see Figure 19), suggesting that also in the Type 2 basin the recirculation between the wave guides is large. Figure 20 shows that this results in current velocities V which deviate significantly from the uniform longshore current velocities.

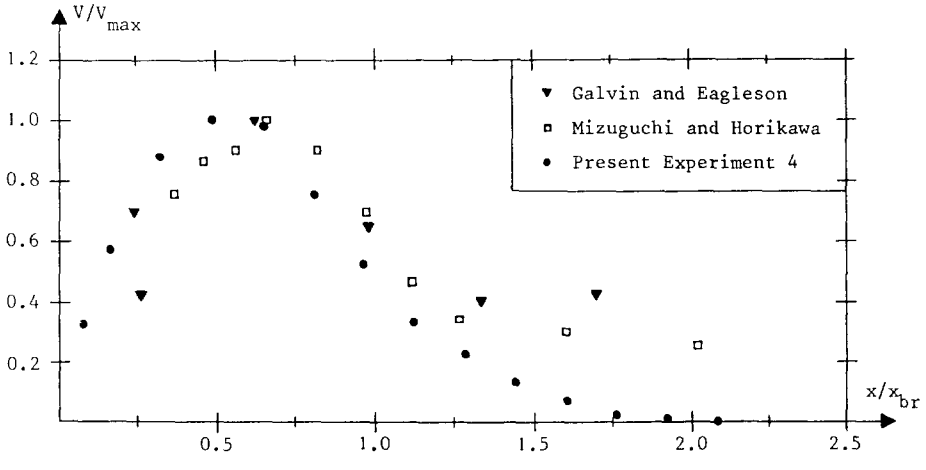

Fig. 18. Cross-sectional distributions of V/V_{max} in Galvin and Eagleson's (1965) Series II Test 8 ($V_{max}=11.3$ cm/s, $x_{br}=42.8$ cm), Mizuguchi and Horikawa's (1978) Case 1 ($V_{max}=17.1$ cm/s, $x_{br}=66.5$ cm) and uniform situation of present Experiment 4 ($V_{max}=40.4$ cm/s, $x_{br}=251$ cm); these data of Galvin and Eagleson and of Mizuguchi and Horikawa were observed in cross-sections located at a distance of about 0.7 of the beach length downstream from the updrift wave guide.

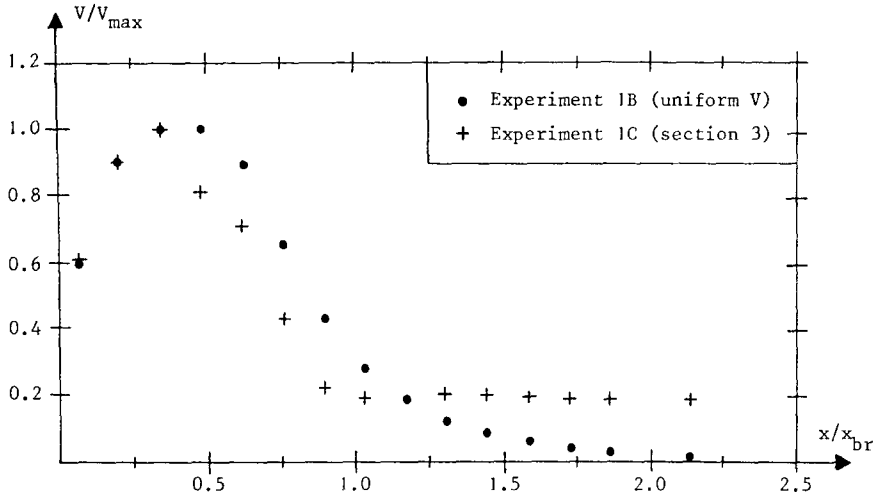

Fig. 19. Cross-sectional distributions of V/V_{max} in Experiment 1C in section 3 (where $V_{max}=55.3$ cm/s and $x_{br}=145$ cm) and in uniform situation of Experiment 1B (in which $V_{max}=66.2$ cm/s and $x_{br}=145$ cm).

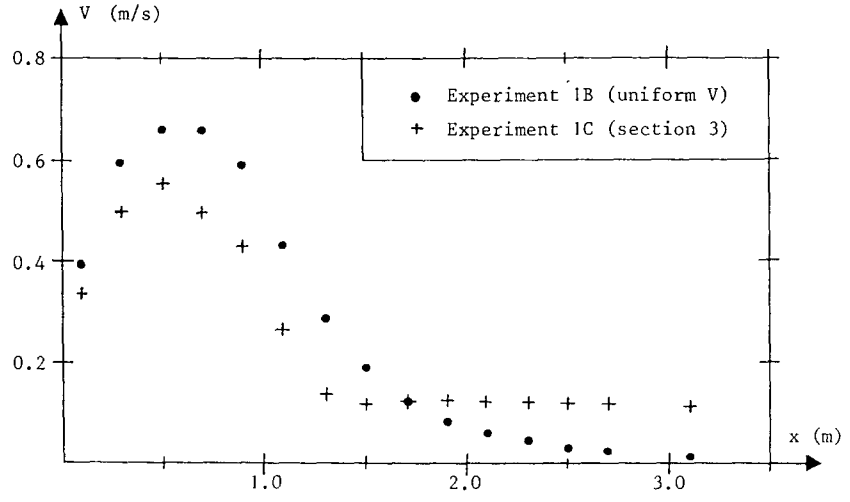

Fig. 20. Cross-sectional distributions of depth-averaged longshore current velocity V in section 3 in Experiment 1C and in uniform situation of Experiment 1B.

The accuracy of the present flow velocity data is good, surprisingly good considering the simple measuring technique: this is mainly due to the large number of observations per measuring point and the great care of the observers.

As already mentioned in the introduction, the present data ara presented in this paper for use by others and not for application in the paper itself. A

comparison of a mathematical longshore current model with the data, see Visser (1984a,b), has indicated that, owing to the rate of detail and accuracy, the present data are very appropriate for such a comparison and can be very helpful in the process of improving theory.

TABLE A-1

$V(x)$, $\bar{V}(x)$, $h(x)$, $H(x)$ and $\theta(x)$ in Experiment 1 for $Q_p = 35$ dm^3/s and $w_d/x_{br} = 1.3$

x (m)	$V(x)$ in (cm/s) in sections				$\bar{V}(x)$ (cm/s)	$h(x)$ (cm)	$H(x)$ (cm)	$\theta(x)$ (degr)
	0	1	2	3				
0.10	39.3	40.7	39.6	38.6	39.6	0.5		
0.30	60.0	58.6	61.3	57.6	59.4	1.5		
0.50	66.6	67.4	66.3	64.3	66.2	2.5	2.9	13.0
0.70	66.8	67.1	66.0	63.8	65.9	3.5	4.8	16.6
0.90	60.9	59.1	59.5	57.4	59.2	4.8	5.7	19.3
1.10	45.4	41.0	43.9	42.3	43.2	6.5	7.5	20.2
1.30	31.4	30.0	27.9	25.4	28.7	8.6	9.8	20.8
1.50	20.9	19.4	17.5	17.5	18.8	10.6	10.3	21.2
1.70	12.8	12.9	11.3	12.5	12.4	12.7	9.6	
1.90	8.3	7.9	8.2	8.7	8.3	14.7	8.3	
2.10	5.7	5.6	6.5	6.0	6.0	16.7	7.4	
2.30	3.9	3.9	4.4	4.1	4.1	18.7	7.5	
2.50	2.2	3.0	3.3	2.6	2.8	20.7	7.7	
2.70	1.5	2.4	2.3	1.5	1.9	22.7	7.9	
3.10	0.1	1.6	1.8	0.9	1.1	26.7	8.2	

TABLE A-2

$V(x)$, $\bar{V}(x)$, $h(x)$, $H(x)$ and $\theta(x)$ in Experiment 2 for $Q_p = 50$ dm^3/s and $w_d/x_{br} = 1.3$

x (m)	$V(x)$ in (cm/s) in sections				$\bar{V}(x)$ (cm/s)	$h(x)$ (cm)	$H(x)$ (cm)	$\theta(x)$ (degr)
	0	1	2	3				
−0.03	0.0	35.1	26.2	25.6	21.7			
0.17	61.2	65.1	60.8	65.3	63.1	1.2		13.6
0.37	71.6	71.2	69.3	71.8	71.0	2.6	2.1	17.6
0.57	73.0	73.8	69.7	71.5	72.0	4.2	3.1	20.7
0.77	67.0	68.1	65.6	67.7	67.1	5.4	4.0	21.8
0.97	55.6	58.7	57.5	58.1	57.5	6.8	5.5	22.8
1.17	43.3	42.7	43.1	42.7	43.0	8.8	8.6	23.3
1.37	32.7	32.6	30.0	31.3	31.6	10.8	9.7	24.1
1.57	23.3	24.3	20.9	23.6	23.0	12.8	9.9	24.5
1.77	14.9	16.4	15.8	16.2	15.8	14.8	9.8	25.0
1.97	10.0	12.2	10.7	10.7	10.9	16.8	9.5	25.5
2.17	6.4	6.8	6.8	6.3	6.6	18.8	9.2	26.0
2.37	4.4	3.6	4.6	4.0	4.2	20.8	9.5	26.0
2.57	1.2	2.3	2.8	2.4	2.2	22.8	9.6	26.0
2.97		0.0	0.7	1.1	0.6	26.8	9.2	26.1

TABLE A-3

$V(x)$, $\bar{V}(x)$, $h(x)$, $H(x)$ and $\theta(x)$ in Experiment 3 for $Q_p = 40$ dm^3/s and $w_d/x_{br} = 1.4$

x (m)	$V(x)$ in (cm/s) in sections				$\bar{V}(x)$ (cm/s)	$h(x)$ (cm)	$H(x)$ (cm)	$\theta(x)$ (degr)
	0	1	2	3				
−0.02	17.7	20.5	16.9	22.6	19.4			
0.18	42.6	41.9	39.3	44.1	42.0	1.2		
0.38	46.5	45.3	45.8	45.6	45.8	2.4	1.8	7.7
0.58	46.8	45.7	48.8	47.2	47.1	3.8	3.1	9.5
0.78	45.5	44.0	46.1	45.6	45.3	5.1	4.8	10.6
0.98	42.0	41.6	42.1	41.8	41.9	6.8	5.5	11.2
1.18	34.6	36.8	34.0	34.0	34.8	8.8	8.5	11.8
1.38	27.1	28.6	25.2	26.2	26.8	10.8	9.4	12.6
1.58	21.7	21.6	18.6	19.4	20.3	12.9	9.3	13.0
1.78	16.2	14.8	13.0	14.0	14.5	15.0	9.2	13.4
1.98	9.4	10.2	8.8	8.9	9.3	17.0	9.0	13.6
2.18	5.7	6.7	5.8	4.9	5.8	19.0	9.2	13.9
2.38	3.5	3.8	4.0	3.6	3.7	21.0	8.7	14.2
2.58	1.8	2.5	2.3	2.6	2.3	23.0	8.3	14.4
2.98		0.5	1.3	0.5	0.8	27.0	9.1	14.6

APPENDIX: MAIN SET OF DATA

The main set of data of the present observations of (virtually) uniform longshore currents is given in the Tables A-1 through A-8. These tables contain the depth-averaged longshore current

TABLE A-4

$V(x)$, $\bar{V}(x)$, $h(x)$, $H(x)$ and $\theta(x)$ in Experiment 4 for $Q_p = 50$ dm^3/s and $w_d/x_{br} = 1.2$

x (m)	$V(x)$ in (cm/s) in sections				$\bar{V}(x)$ (cm/s)	$h(x)$ (cm)	$H(x)$ (cm)	$\theta(x)$ (degr)
	0	1	2	3				
0.01	0.0	0.0	0.0	0.0	0.0	0.0		
0.21	12.2	14.0	8.9	18.2	13.3	0.9		
0.41	24.5	22.7	18.8	27.0	23.2	1.8		
0.81	37.4	33.0	33.5	37.6	35.4	3.7	1.6	
1.21	42.8	37.6	40.2	40.8	40.4	5.3	2.6	
1.61	41.6	36.2	38.8	40.9	39.4	6.9	3.4	
2.01	32.0	30.2	29.9	29.7	30.4	8.5	5.6	11.4
2.41	21.1	23.2	20.3	19.8	21.1	10.5	8.6	12.5
2.81	12.1	13.9	14.0	13.6	13.4	12.4	8.4	13.1
3.21	6.8	9.7	10.0	9.9	9.1	14.5	7.8	13.5
3.61	3.4	6.4	6.2	5.3	5.3	16.6	8.0	13.7
4.01	1.7	3.9	2.8	2.2	2.7	18.6	7.9	13.9
4.41	0.6	2.4	0.7	0.7	1.1	20.6	7.6	14.2
4.81	0.3	1.1	0.3	0.2	0.5	22.6	7.6	14.3
5.21		−0.1	0.1	−0.3	−0.1	24.6	7.5	14.4

TABLE A-5

$V(x)$, $\bar{V}(x)$, $h(x)$, $H(x)$ and $\theta(x)$ in Experiment 5 for $Q_p = 65$ dm^3/s and $w_d/x_{br} = 1.3$

x (m)	$V(x)$ in (cm/s) in sections			$\bar{V}(x)$ (cm/s)	$h(x)$ (cm)	$H(x)$ (cm)	$\theta(x)$ (degr)
	0	1	2				
0.12	10.8	8.5	11.6	10.3	0.8		
0.32	18.0	17.8	19.0	18.3	1.5		
0.52	25.5	27.6	25.0	26.0	2.2		
0.92	37.0	35.8	37.7	36.8	3.7	2.2	7.2
1.32	41.4	40.4	40.2	40.7	5.1	3.3	9.1
1.72	41.4	39.7	39.3	40.1	6.5	4.5	9.9
2.12	34.2	32.1	35.4	33.9	8.3	6.4	10.7
2.52	25.8	25.8	27.9	26.5	10.3	10.0	12.0
2.92	19.0	18.5	18.8	18.8	12.3	10.8	12.4
3.32	12.3	11.2	10.4	11.3	14.3	10.4	12.7
3.72	6.6	6.9	5.2	6.2	16.4	9.7	12.8
4.12	3.2	3.1	2.2	2.8	18.4	9.0	12.9
4.52	1.2	1.5	0.9	1.2	20.4	8.7	
4.92	0.5	1.0	0.5	0.7	22.4	8.3	
5.32	−0.2	0.8	0.4	0.3	24.4	7.8	

velocities V in the different sections as function of the on–offshore parameter x ($x = 0$ at the wave set-up line), the alongshore averaged (over sections 0 or 1 through 2 or 3) longshore current velocities $\bar{V}(x)$, the mean water depths $h(x)$ and wave heights ($H(x)$ averaged over sections 1 and 2 and the angles of incidence $\theta(x)$.

TABLE A-6

$V(x)$, $\bar{V}(x)$, $h(x)$, $H(x)$ and $\theta(x)$ in Experiment 6 for $Q_p = 30$ dm^3/s and $w_d/x_{br} = 1.35$

x (m)	$V(x)$ in (cm/s) in sections			$\bar{V}(x)$ (cm/s)	$h(x)$ (cm)	$H(x)$ (cm)	$\theta(x)$ (degr)
	0	1	2				
0.10	4.6	2.3	7.0	4.6	0.4		
0.30	15.9	15.4	21.2	17.5	1.3		
0.50	26.2	26.4	25.7	26.1	2.3	0.8	
0.70	31.4	29.9	31.0	30.8	3.3	1.3	
1.10	33.5	31.8	30.7	32.0	4.9	2.2	11.2
1.50	27.7	26.6	24.8	26.4	6.6	4.1	12.1
1.90	17.2	18.6	17.5	17.8	8.6	5.5	13.1
2.30	10.3	11.2	11.1	10.9	10.6	5.2	13.7
2.70	6.7	7.0	7.6	7.1	12.6	5.4	14.2
3.10	4.1	4.0	5.4	4.5	14.7	5.5	14.3
3.50	2.8	2.7	3.3	2.9	16.7	5.4	
3.90	1.1	1.4	2.1	1.5	18.7	5.5	
4.30	0.8	0.8	1.2	0.9	20.7	5.6	
4.70		0.7	0.2	0.4	22.7	5.8	
5.10		0.4	−0.1	0.1	24.8	5.7	

TABLE A-7

$V(x)$, $\bar{V}(x)$, $h(x)$, $H(x)$ and $\theta(x)$ in Experiment 7 for $Q_p = 20$ dm^3/s and $w_d/x_{br} = 0.9$; $h(x)$ adopted from Experiment 4

x (m)	$V(x)$ in (cm/s) in sections			$\bar{V}(x)$ (cm/s)	$h(x)$ (cm)	$H(x)$ (cm)	$\theta(x)$ (degr)
	1	2	3				
0.10	0.0	0.0	0.0	0.0	0.4		
0.30	5.3	6.8	4.2	5.4	1.4		4.6
0.50	9.2	11.3	8.2	9.6	2.3		
0.70	15.4	14.2	15.0	14.9	3.3	1.1	6.7
1.10	18.8	19.9	20.0	19.6	4.9	2.0	8.3
1.50	19.7	20.6	22.0	20.8	6.5	2.9	9.9
1.90	17.8	16.6	17.9	17.4	8.1	4.1	11.1
2.30	12.7	11.4	12.0	12.0	10.0	6.0	12.0
2.70	6.9	6.4	6.6	6.6	12.0	8.9	12.8
3.10	4.1	4.0	4.0	4.0	14.1		12.9
3.50	2.0	2.8	2.4	2.4	16.1		13.1
3.90	1.0	1.6	1.9	1.5	18.1		13.5
4.30	0.6	1.3	0.9	0.9	20.2		13.9
4.70	−0.1	0.6	0.0	0.2	22.2		14.0
5.10	−0.4	−0.4	−0.3	−0.4	24.2		

TABLE A-8

$V(x)$ in section 2 and $h(x)$ in Experiment 8 for $Q_p = 25$ dm^3/s and $w_d/x_{br} = 1.2$; $h(x)$ adopted from Experiment 5

x (m)	$V(x)$ (cm/s)	$h(x)$ (cm)
0.10	0.0	0.4
0.30	2.0	1.1
0.50	6.5	1.9
0.70	11.6	2.6
0.90	13.8	3.5
1.30	16.7	4.9
1.70	15.9	6.3
2.10	14.3	8.1
2.50	10.4	10.1
2.90	6.4	12.1
3.30	5.9	14.1
3.70	4.2	16.2
4.10	2.9	18.2
4.50	1.8	20.2
4.90	1.0	22.2

ACKNOWLEDGEMENTS

The author would like to thank J.A. Battjes and C.J. Galvin for their critical comment to the manuscript.

REFERENCES

Basco, D.R., 1982. Surfzone currents. U.S. Army Coastal Eng. Res. Cent., Misc. Rep. 82-7, 336 pp.

Basco, D.R., 1983. Surfzone currents. Coastal Eng., 7: 331–355.

Battjes, J.A., 1972. Set-up due to irregular waves. Proc. 13th Int. Conf. Coastal Eng., Vancouver, pp. 1993–2004.

Battjes, J.A., 1974. Computation of set-up, longshore currents, run-up and overtopping due to wind-generated waves. Comm. on Hydraulics, Rep. 74-2, Dep. of Civil Eng., Delft Univ. of Technology, Delft, The Netherlands, 244 pp.

Battjes, J.A., 1988. Surf-zone dynamics. Annu. Rev. Fluid Mech., 20: 257–293.

Brebner, A. and Kamphuis, J.W., 1963. Model tests on the relationship between deep-water wave characteristics and longshore currents. Civil Eng. Res. Rep. 31, Queens University, Kingston, Ontario, Canada, 28 pp.

Dalrymple, R.A. and Dean, R.G., 1972. The spiral wavemaker for littoral drift studies. Proc. 13th Int. Conf. Coastal Eng., Vancouver, pp. 689–705.

Dalrymple, R.A., Eubanks, R.A. and Birkemeier, W.A., 1977. Wave-induced circulation in shallow basins. J. Waterway, Port, Coastal Ocean Div., A.S.C.E., 103: 117–135.

Delft Hydraulics Laboratory, 1977. Water motion in a coastal model with a fixed bottom (in Dutch). T.O.W. Rep. M 918 part 4, Delft, The Netherlands.

Galvin, C.J., 1967. Longshore current velocity: a review of theory and data. Rev. Geophys., 5: 287–304.

Galvin, C.J., 1968. Breaker type classification on three laboratory beaches. J. Geophys. Res., 73: 3651–3659.

Galvin, C.J. and Eagleson, P.S., 1965. Experimental study of longshore currents on a plane beach. U.S. Army Coastal Eng. Res. Cent., Tech. Mem. 10, 80 pp.

Hansen, J.B. and Svendsen, I.A., 1979. Regular waves in shoaling water, experimental data. Series Paper 21, Inst. Hydrodyn. and Hydraulic Eng., Techn. Univ. of Denmark, Lyngby, Denmark.

Kamphuis, J.W., 1977. Discussion on wave-induced circulation in shallow basins. J. Waterway Port Coastal Ocean Div., ASCE, 103: 570–571.

Kim, K.H., Sawaragi, T. and Deguchi, I., 1986. Lateral mixing and wave direction in the wave-current interaction region. Proc. 20th Int. Conf. Coastal Eng., Taipei, pp. 366–380.

Komar, P.D., 1975. Nearshore currents: generation by obliquely incident waves and longshore variations in breaker heights. In: J. Hails and A. Carr (Editors), Nearshore Sediment Dynamics and Sedimentation. Wiley, London, pp. 17–45.

Kraus, N.C. and Sasaki, T.O., 1979. Influence of wave angle and lateral mixing on the longshore current. Mar. Sci. Common., 5: 99–126.

Longuet-Higgins, M.S., 1972. Recent progress in the study of longshore currents. In: R.E. Meyer (Editor), Waves on Beaches and Resulting Sediment Transport. Academic Press, New York, N.Y., pp. 203–248.

Longuet-Higgins, M.S. and Stewart, R.W., 1960. Changes in the form of short gravity waves on long waves and tidal currents. J. Fluid Mech., 8: 565–583.

Longuet-Higgins, M.S. and Stewart, R.W., 1964. Radiation stresses in water waves; a physical discussion with applications. Deep-Sea Res., 11: 529–562.

Mizuguchi, M. and Horikawa, K., 1978. Experimental study on longshore current velocity distribution. Bull. Fac. Sci. Eng., Chuo Univ., Tokyo, Japan, 21: 123–150.

Phillips, O.M., 1966. The dynamics of the upper ocean. Cambridge University Press, Cambridge, 2nd ed., 1977, 336 pp.

Putnam, J.A., Munk, W.H. and Traylor, M.A., 1949. The prediction of longshore currents. Trans. Am. Geophys. Union, 30: 337–345.

Seymour, R.J. and Gable, C.G., 1980. Nearshore Sediment Transport Study Experiments. Proc. 17th Int. Conf. Coastal Eng., Sydney, pp. 1402–1415.

Singamsetti, S.R. and Wind, H.G., 1980. Breaking waves: characteristics of shoaling and breaking waves normally incident to plane beaches of constant slope. T.O.W. Rep. M1371, Delft Hydr. Lab., Delft, The Netherlands, 157 pp.

Stive, M.J.F., 1984. Energy dissipation in waves breaking on gentle slopes. Coastal Engineering, 8: 99–127.

Svendsen, I.A., 1984. Wave heights and set-up in a surf zone. Coastal Engineering, 8: 303–329.

Svendsen, I.A. and Hansen, J.B., 1977. The wave height variation for regular waves in shoaling water. Coastal Eng., 1: 261–284.

Svendsen, I.A. and Lorenz, R.S., 1989. Velocities in combined undertow and longshore currents. Coastal Eng., 13: 55–79.

Visser, P.J., 1980. Longshore current flows in a wave basin. Proc. 17th Int. Conf. Coastal Eng., Sydney, pp. 462–479.

Visser, P.J., 1982. The proper longshore current in a wave basin. Comm. on Hydraulics Rep. 82-1, Dep. Civil Eng., Delft Univ. of Technology, Delft, The Netherlands, 86 pp.

Visser, P.J., 1984a. A mathematical model of uniform longshore currents and the comparison with laboratory data. Comm. on Hydraulics, Rep. 84-2, Dep. Civil Eng., Delft Univ. of Technology, Delft, The Netherlands, 151 pp.

Visser, P.J., 1984b. Uniform longshore current measurements and calculations. Proc. 19th Int. Conf. Coastal Eng., Houston, pp. 2192–2207.